ОБЪЕДИНЕННЫЙ
ИНСТИТУТ
ЯДЕРНЫХ
ИССЛЕДОВАНИЙ

Дубна

E4 - 5350

H. Schulz, H.J. Wiebicke, R. Fülle, D. Netzband,
K. Schlott

ЛАБОРАТОРИЯ ТЕОРЕТИЧЕСКОЙ ФИЗИКИ

# A GENERALIZED DWBA MODEL APPLIED TO THE $^{24}$Mg (dp) $^{25}$Mg REACTION AT $E_d$ = 13.5 MeV

1970

E4 - 5350

**H. Schulz, H.J. Wiebicke, R. Fülle,* D. Netzband,***
**K. Schlott ***

# A GENERALIZED DWBA MODEL APPLIED TO THE $^{24}$Mg (dp) $^{25}$Mg REACTION AT $E_d$ = 13.5 MeV

Submitted to Nucl. Phys.

* Central Institute for Nuclear Research, Rossendorf near Dresden , GDR.

## I. Introduction

The most widely used method for describing stripping reactions is the distorted wave Born approximation (DWBA). In the DWBA the transition is assumed to take place directly from the entrance to the exit channel without any excitation of internal variables of the target and residual nuclei. But if there are low-lying collective states the inelastic excitation may well play some role. In such cases the usual DWBA can hardly describe the measurements. Therefore, it is necessary to include inelastic excitations by generalizing the distorted waves. To this problem many works have been related [1-6]. In particular Iano and Austern [3] expanded the stripping amplitude in terms of the deformation parameter. They were able to investigate the interference of the direct and indirect transitions without calculating the generalized distorted waves.

In previous papers [4,7] the generalized distorted waves have been calculated by means of a coupled channels procedure. In a forthcoming paper [8] a detailed comparison of this method with that of Iano and Austern and with experimental data will be given. A methodically very similar consideration was made by Iano, Penny between $5^{\circ}$ and $175^{\circ}$ at $E_d = 10.1$ MeV with high resolution for 44 angular distributions represented in arbitrary units. At the Rossendorf cyclotron 10 angular distributions between $5^{\circ}$ and $160^{\circ}$ were measured with Li-drifted detectors at $E_d = 13.5$ MeV /12/. Further references are quoted in /10/, /11/ and /12/.

The angular distributions measured in Rossendorf belong to the transitions leading to the levels displayed in fig. 1. This level scheme was taken from /13/. Only for the weak transitions the errors reach about 10%, for the others they are within the diameters of the circles in the figures. The calibration error of the absolute value amounts to about 20% for each point.

The closed lying levels were not resolved. These levels are joined in fig. 1. by brackets. But from /10/, /11/ and /12/ it is known, that the transitions to the $3/2\ 1/2^+$ [200], $3/2\ 1/2^-$ [330], $7/2\ 1/2^-$ [330], and $1/2\ 1/2^-$ [330] levels dominate in the multiplet (see table 1.). The groups leading to the states at 3.399 MeV and 3.408 MeV were never resolved in angular distribution measurements of the (d,p)-reaction.

## 3. Optical Parameters and Scattering Data

As it is well known the theoretical differential cross sections are strongly affected by the optical parameters. A critical examination of the theory used to describe the (d,p)-reaction can be carried out only if the uncertainties in the parameters are removed as far as possible. Therefore, the optical and deformation parameters have to be adjusted from the experimental data of the elastic and inelastic scattering of deuterons and protons. For this purpose the code KASTOR (written by H.S. and H.J.W.) was used. It

is described in detail and applied to experimental data in [8,14,15].
This code takes into account all the orders of the deformation parameters $\beta_2$ and $\beta_4$ and allows to fit all at once several differential cross sections belonging to the ground state rotational band.
It makes use of the adiabatic approximation [16] and containes no spin-orbit coupling.

The deuteron scattering data were taken from [12]. The first $0^+$ and $2^+$ state in $^{25}Mg$ were measured also at $E_d = 13.5$ MeV with surface barrier detectors using the thin detector technique and an enriched target. Since the $4^+$ group is sitting on the proton edge and was not clearly separated from the second $2^+$ level, a search for the deformation parameters $\beta_2$ and $\beta_4$ was impossible in any case. Therefore, the experimental scattering data were fitted at fixed values of $\beta_2$ and $\beta_4$ found by the proton scattering on $^{24}Mg$ and sicussed below. The obtained optical parameters for the deformed Saxon-Woods potential are compiled in table 2. The radii $r_v$ and $r_c$ were used as fixed parameters. The experimental data and the results of the fit are shown in fig. 2. Besides the missing peak at $115^{\circ}$ in the elastic scattering and some smaller differences for the $2^+$ level the experiments are fitted quite well with reasonable parameters. The missing peak could be obtained for $\beta_2 \approx 0.3$ only but entailing that the inelastic scattering at large angles comes completely out of phase.

At the incident energy $E_d = 13.5$ MeV the proton centre mass energy depending on the $Q$-value reaches from 14 up to 17.5 MeV. For $E_p = 17.5$ MeV Grawley measured the elastic and inelastic scattering of protons on several 2s 1d nuclei [17].
His data for the scattering on $^{24}Mg$ were analysed by de Swiniarsky et al. [18] with a coupled channel calculation. They found

proton parameters which fit Grawley's data excellently, as shown in fig. 3. The curves in fig. 3 were calculated with the code KASTOR. The used parameters are compiled in table 2. The fig. 3 illustrates the influence of $\beta_4$. We believe that the proton parameters found for $^{24}Mg$ hold for the outgoing channel ($^{25}Mg + p$) of the (d, p) reaction too, all the more as Antropov et al. /14/ were able to reproduce the inelastic deuteron scattering at $E_a = 12.1$ MeV on all Mg isotopes with optical parameters very similar for each isotope.

The same deformation parameters $\beta_2$ and $\beta_4$ extracted from the inelastic proton scattering on $^{24}Mg$ were used for the deuteron scattering and for the (d, p) reaction too, because the available $2^+$ and $4^+$ states in the inelastic proton scattering permit to adjust the deformation parameters $\beta_2$ and $\beta_4$ much better than in the inelastic deuteron scattering.

## 4. Calculation of the Stripping Differential Cross Section

For the comparison with the experimental data the angular distributions of four rotational bands in $^{25}Mg$ were calculated with the computer code POLLUX. This code written by H.S. and H.J.W. calculates the differential cross sections of one-nucleon transfer reactions on deformed nuclei. The generalized distorted waves were obtained by a coupled channels procedure using the adiabatic approximation and taking into account indirect contributions by inelastic excitation of the low-lying rotational levels of the target and final nuclei. A more detailed description of the code

POLLUX is made in [9]. There can be found comparisons to the results of other models and to several experimental data too.

### 4.1. The Single-Particle Function for Transferred Nucleon

The bound state function of the transferred paricle used in the code POLLUX is calculated in a deformed single-particle potential of the Saxon-Woods type and expanded in terms of spherical basis functions $R_{nlj}(r)$ [19]

$$\phi_{\Omega} = \sum_{n\ell j\Lambda} C^{(\Omega)}_{n\ell j} R_{n\ell j}(r)(\ell s_n \Lambda \Omega - \Lambda \mid j \Omega) Y_{\ell\Lambda}(\hat{r}) X_{s_n \Omega - \Lambda}, \qquad (1)$$

where $Y_{\ell\Lambda}(\hat{r})$ are the spherical and $X_{s_n \Omega-\Lambda}$ the spin functions. The expansion coefficients $C^{(\Omega)}_{n\ell j}$ depend on the deformation and were obtained with the aid of a computer code written by Gareev and Ivanova[x].

The radial basis functions $R_{n\ell j}(r)$ were numerically calculated with the potential parameters $r_0 = 1.25$ fm and $a = 0.65$ fm. The potential deep $V = 47$ MeV was adjusted to give the proper neutron binding energy $E_n = 7.33$ MeV, A spinorbit strength of $V_{so} = 4$ MeV yielded the right energy level scheme.

Obviously, the deformation parameter for the single-particle wave function should have the same value as extracted by fitting the inelastic scattering data. To avoid the uncertainties which could arise from this adequacy the deformation parameter in

---

[x] We are indepted to Dr. F.A. Gareev and Mrs. S.P. Ivanova for making their code available to us.

the single-particle wave function has been varied. The coefficients for $\beta_2 = 0.45$ and $\beta_2 = 0.35$ are shown in table 5. A hexadecupole deformation $\beta_4$ was not considered. We see that the deformation dependence of the $C_{n\ell j}$ is weak and with the exception of the $C_{2s_{1/2}}$ [211] the deviation for the most important coefficients is smaller than 10%. Therefore, we have given only for the band $1/2^+$ [211] the curves belonging to the both values $\beta_2 = 0.45$ and $\beta_2 = 0.35$. For all other curves the value $\beta_2 = 0.45$ was taken.

For a comparison Nilsson's coefficients /20/ in the $\ell j$ -representation at $\beta_2 = 0.3$ and those calculated by Rost's coupled channels code /20/ and given by Dehnhardt and Intema /13/ are also quoted in table 3. As is seen the values of the corresponding coefficients are mutually very similar. That can be expected because in the light nuclei the oscillator potential as well as the Saxon-Woods potential are a good approximation to describe the single-particle levels.

Rost's code is able to consider quasi stationary states and in /13/ the coefficients of these states with $N = 4$ from the g -shell are given also. Because of the strong energy distance they are not important. The negative parity rotational band $1/2^-$ [330] has an excitation energy of $E_{ex} = 3.4$ MeV and the spherical basis states of the 2p 1f - shell are partly not bound in the potential with the parameters given above. Therefore, a comparison of the coefficients with those of the Nilsson model is difficult. Nevetherless ,the most important states are bound and have very similar coefficients.

## 4.2. Comparison with the Experimental Data and Discussion

In calculating the theoretical differential cross sections no parameters have been varied. Also no renormalization of the theoretically predicted curves to the experimental data was made in the corresponding figures 4 - 6 and 8. Instead of it in table 4 are compiled the interesting ratios of calculated to measured differential cross sections at two angles in the forward and backward angle region. These ratios have the same uncertainties of 20% as the experimental data.

### 4.21. The $5/2^+$ [202] Ground State Band

Our results are shown in fig. 4. The angular distribution for the transition to the $5/2^+$ ground state is described very well up to backward angles. The agreement with the experimental data is much better than for all other levels. The transitions to higher lying members of the band are stripping forbidden. That means that only indirect terms contribute in the transition amplitude. Therefore, the theoretical description of the angular distibution of these transitions is a sensitive test for the used model. Two higher lying states were identified but only the $7/2^+$ could be resolved. The general behaviour of its calculated angular distribution sufficiently corresponds to that of the experimental data. Our prediction is too small by a factor of 0.3. The slope at backward angles is too strong.

### 4.22. The $1/2^+$ [211] and $1/2^+$ [200] Bands

Since the theoretical predictions for these two bands are affected only by the different $C_{n\ell j}^{(\Omega)}$ coefficients and the Q-value it is particularly interesting to discuss them together.

a) The $J = 1/2$ states: The both measured and all the calculated angular distributions are very similar. That is seen in figs. 5 and 6. The general behaviour is reproduced, but the calculated curves have rather deep tips probably caused by the missing spin-orbit coupling.

For the comparison between the two bands we consider the ratios of the corresponding differential cross sections

$$R = \frac{d\sigma}{d\Omega} (J\, 1/2^+ [211]) / \frac{d\sigma}{d\Omega} (J\, 1/2^+ [200]) \; . \tag{2}$$

From Satchler's formalism/22/ the cross section is expected to be proportional to $(C^{(\Omega)}_{n\ell j})^2$ with $j = J$ and the expression (2) becomes to

$$R_s = (C_{n\ell j} [211] / C_{n\ell j} [200])^2 \tag{3}$$

in this theory. The difference between the values $R_s$ and our calculated ones $R$ illustrates the influence of the other terms with $j \neq J$ not considered in/22/. For the $J = 1/2$ states this influence is small. We obtained at the two values of the deformation parameter $\beta_2$ used in the bound state function the ratios

$$R_s(\beta_2 = 0{,}45) = 0{,}50 \, , \quad R(\beta_2 = 0{,}35) = 0{,}47$$

and for $R$ the samewhat angular depending values

$$R(\beta_2 = 0{,}45) = 0{,}28 \ldots 0{,}23 \, , \; R(\beta_2 = 0{,}35) = 0{,}45 \ldots 0{,}37 \, .$$

These values are very different from the ratio of the corresponding experimental differential cross sections $R_{exp} \approx 3.3$ and our model gives for the $J = 1/2$ states no improvement in comparison with Satchler's theory. The proportionality of the differential cross sections to $(C^{(\Omega)}_{n\ell j})^2$ in this case permits to determine the so-called "experimental coefficient"

$$C_{2s\,1/2}[211] \approx (\pm)\,0{,}75 \text{ and } C_{2s\,1/2}[200] \approx (\pm)\,0{,}40$$

which can not be obtained within the usual single particle models.

b) The $J = 3/2$ states: In our measurement the state 3/2 $1/2^+$ [200] is not resolved from the 7/2 $1/2^+$ [211] level. However from /10/ at $E_d = 15$ MeV and from /11/ at $E_d = 10$ MeV it is sure that the contribution of the 7/2 $1/2^+$ [211] state is almost negligible in the forward region. That is expressed by the intensity ratios in table 1. In figs. 5 and 6 are shown our results. Both measurements look similar and $R_{exp} = 0.9... 0.8$ is found. The corresponding theoretical ratios $R_s$ with $n\ell j = 1d3/2$ are

$$R_s(\beta_2 = 0{,}45) = 1{,}69\,, \quad R_s(\beta_2 = 0{,}35) = 1{,}29\,.$$

For the ratios $R$ we obtained

$$R(\beta_2 = 0{,}45) = 1{,}1 \ldots 0{,}6\,, \quad R(\beta_2 = 0{,}35) = 0{,}8 \ldots 0{,}6$$

which agree much better with $R_{exp}$ than $R_s$. The difference between the values of $R$ and $R_s$ illustrate the strong influence of the indirect contributions on the $J = 3/2$ states mainly caused by the great $C_{2s\,1/2}$ coefficients. The ratios between the calculated and measured differential cross sections in table 4 and figs. 5 and 6 show a quite well agreement in the forward angle region. The opposite sign of the $C_{2s1/2}$ coefficients in both bands causes the difference in the fluctuation of the calculated curves according to the experimental angular distribution.

c) The $J = 5/2$ states: For the 1/2 [200] band this level was not resolved. The theoretical curves are very different for both bands because the corresponding coefficients $C_{1d5/2}$ are small and the influence of the $j \neq J$ terms is strong. The smooth behaviour of the experimental angular distribution of the 5/2 $1/2^+$ [211] is quite well reproduced.

d) The $J$-dependence of the cross sections: illustrating the $J$-dependence of the cross sections all calculated angular distributions with the same transferred angular momentum $L = 2$ are represented in fig. 7. The curves have been normalized to each other at $\theta_{C.M.} = 25^{\circ}$. As is seen the $J$-dependence of the cross section is remarkable, and mainly, the results of the consideration of the indirect transitions by means of the generalized distorted waves. It seems to us worthwile to point at the essentially improved agreement attained by the strong $J$-dependence for the $J = 3/2$ and $J = 5/2$ states of the $1/2^+$ [211] band, for instance.

e) The $J = 7/2$ state: For the $1/2^+$ [200] band this state is not yet identified. The 7/2 $1/2^+$ [211] level was again not resolved in /12/. The transition to this state is stripping forbidden and therefore it would be interesting if it should be resolved.

## 4.23. The $1/2^-$ [330] Band

A critical investigation of the negative parity $1/2^-$ [330] band is more difficult, because its spherical basis states are partly unbound in the single-particle potential given in chapt. 4.1.

The influence of these unbound states seems to be important, but they can not be involved in the present program. The bound basis states have small binding energies which depend sensitivly on the potential parameters. Therefore the theoretical predictions for this band have more uncertainties as for the other bands.

In particular, the 2p1/2 basis state was not bound in the potential under consideration. But it is important because only the 2p1/2 state permits the direct transition to the $1/2^-$ rotational level. A test calculation neglecting the 2p1/2 state yielded a theoretical curve completely diverging from the experimental data. Therefore, we tried to appreciate the influence of this state by admitting that it is formally a bound state with an energy 0.2 MeV. For this purpose a potential deep $V = 55.6$ MeV is necessary. To avoid the same difficulties in the calculation of the expansion coefficients the Nilsson coefficients at the deformation $\beta_2 = 0.3$ were used.

Our theoretical predictions are shown in fig. 8. The $J = 1/2$, $3/2$ states have a typical $L = 1$ behaviour. Comparing both curves at small angles we can establish a good proportionality of the cross section to the corresponding coefficients $(C^{(\Omega)}_{n\ell j})^2$ with $j=J$. That means the indirect terms arising from the 1f basis states are small in spite of a very important $C_{1f\,7/2}$ -coefficient.

Comparing our results with the experimental data we must remember that all states of this band were not resolved in the measurement from other states. The 4.351 MeV level mixing to the $1/2^-$ state has not yet been classified. The 9/2 $5/2^+$ [202] level mixing to the $3/2^-$ state is negligible for small angles (see table 1). In the backward angle region the calculated cross sections are comparable and the sum of both curves give a better agreement with the measurement.

Still more complicated is the analysis of the $7/2^-$ state, because it is mixed with two other states, the one of them at 4.055 MeV has not been classified and the second one (5/2 $1/2^+$ [ 200 ] ) in contradiction to the data in table 1 has the same order of magnitude as the $7/2^-$ state. Nevetherless, the calculation reproduces the general shape of the measured angular distribution. The sum of the two known states (upper curve) agrees sufficiently well with the absolute values of the cross section, also.

## 5. Summary

The experimental material displayed in the present work has given the possibility to investigate all known rotational bands in the final nuclei $^{25}Mg$ . For the analysis of the experimental differential cross sections a generalized DWBA model for one-nucleon transfer reactions on deformed nuclei was used. Since we adjusted the optical and deformation parameters from the elastic and inelastic scattering and calculated the bound state function in the framework of the deformed Saxon-Woods potential, the general uncertainties at the choice of parameters are reduced so far as possible.

The generalized DWBA model has given differential cross sections which sufficiently well agree with the experimental data, in particular for small angles. For angles greater than $120^{\circ}$ the calculated values are generally too small. For transitions with the transferred angular momentum $L=0, 1$ ,the influence of the indirect contributions caused by intermediate excitations of rotational levels is not important and the angular distributions are determibed mainly by the direct terms with $j=J$ . In such cases the deviations of our calculated curves from those predicted by the usual DWBA theory arise from the inclusion of the deformed optical potentials at the calculations of the distorted waves. The transitions with a transferred angular momentum $L \geq 2$ are more influenced by indirect contributions due to the terms with $l < L$. That leads to a strong dependence of the differential cross sections on the transferred spin J . In case of the $L = 2$ transitions the same dependence has been observed in the experimental angular distributions, so that the agreement between the calculated and measured differential cross sections could be improved. By the used generalized DWBA model the stripping forbidden transitions can be explained and the single one resolved in the present experiment has been reproduced suffiently well.

## Acknowledgement

We are deeply indepted to Prof. V.G. Soloviev and Prof. J. Schintlmeister for their continuous interest and for the whole hearty support. One of us (D.N.) would like to acknowledge the important support by the Ministerium fuer Wissenschaft und Technik in Berlin and by the Joint Institute for Nuclear Research in Dubna.

## References

1. S.K. Penny and G.R. Satchler. Nucl.Phys., 53, 145 (1964).
2. B. Kozlowsky and A.de-Shalit. Nucl.Phys., 77, 215 (1966). F.S. Levin. Phys.Rev., 147, 715 (1966).
3. P.J. Iano and N. Austern. Phys.Rev., 151, 853 (1966).
4. V.K. Lukyanov and I.Zh. Petkov. Yadernaya Fizika, 6, 988 (1967).

5. P.D. Kunz, E. Rost and R.R. Johnson. Phys.Rev., 177, 1737 (1969).

6. P.J. Iano, S.K. Penny and R.M. Drisko. Nucl.Phys., A127, 47 (1969).

7. H. Schulz. and H.J. Wiebicke. Phys.Lett., 29B , 18 (1969).

8. V.K. Lukyanov, H. Schulz, and H.J. Wiebicke. To be published in Nucl. Phys.

9. K. Hosono. J.Phys.Soc of Japan, 25, 36 (1968).

10. B. Cujec. Phys.Rev., 136, S1305 (1964).

11. R. Middeleton, H. Hinds. Nucl.Phys., 34, 404 (1962).

12. R. Fülle et al. To be published in a report of the Central Institute for Nuclear Research, Rossendorf, GDR.

13. D. Dehnhard and J.L. Yntema. Phys.Rev., 160, 964 (1967).

14. A.E. Antropov, P.P. Sarubin, B.N. Orlov, H.J. Wiebicke, H.Schulz. Proceedings of the XX Conference of Nuclear Spectroscopy and Nuclear Structure, Leningrad (1970).

15. H.J. Wiebicke, H. Schulz, A.B. Kurepin. Proceedings of the XX Conference of Nuclear Spectroscopy and Nuclear Structure, Leningrad (1970).

16. S.I. Drozdov. Yadernaya Fizika, 5, 786 (1965).

17. O.M. Crawley. Thesis, Princeton University, 1965.
O.M. Crawley and G.T. Garvey. Phys.Rev., 160, 981 (1967).

18. R. de Swiniarski et al. Phys.Rev.Lett., 23, 317 (1969).

19. F.A. Gareev, S.P. Ivanova, and B.N. Kalinkin. Preprints P4-2976 and P4-3451, Dubna (1967).

20. S.G. Nilsson. Det. Kgl. Den. Vid. Selsk., 29, No. 16.

21. E. Rost. Phys.Rev., 154, 994 (1967).

22. G.R. Satchler. Ann. Phys., (N.Y.), 3, 275 (1963).

Received by Publishing Department
on August 10, 1970.

Table 1

Intensity ratios of measured differential cross sections to states unresolved in the present experiment

| unresolved states | angle | $\frac{d\sigma}{d\Omega}(I) : \frac{d\sigma}{d\Omega}(II)$ | ref. |
|---|---|---|---|
| I: 3/2 $1/2^+$ [200] | $25^0$ | 28 : 1 | /10/ |
| | $30^0$ | 18 : 1 | |
| II: 7/2 $1/2^+$ [211] | $130^0$ | 14 : 1 | /11/ |
| I: 3/2 $1/2^-$ [330] | $30^0$ | 33 : 1 | /11/ |
| II: 9/2 $5/2^+$ [202] | $90^0$ | 10 : 1 | |
| I: 7/2 $1/2^-$ [330] | $25^0$ | 40 : 1 | /10/ |
| | $30^0$ | 10 : 1 | |
| II: 5/2 $1/2^+$ [200] | $110^0$ | 2.3 : 1 | /11/ |

Table 2

Values of deuteron and proton parameters found by the elastic and inelastic scattering analysis and used for the calculation of the differential stripping cross section

| particle | $V$ in MeV | $r_V$ in fm | $a_V$ in fm | $W_D$ in MeV | $r_W$ in fm | $a_W$ in fm | $r_C$ in fm | $\beta_2$ (expt) | $\beta_4$ (expt) |
|---|---|---|---|---|---|---|---|---|---|
| d | 80.0 | 1.25 | 0.77 | 17.0 | 1.67 | 0.43 | 1.30 | +0.47 | -0.05 |
| p | 46.0 | 1.22 | 0.60 | 3.60 | 1.27 | 0.64 | 1.22 | +0.47 | -0.05 |

Table 3

Expansion coefficients $C_{n\ell j}^{(\Omega)}$ used in the present work compared to those obtained by Rost's code and to the Nilsson's coefficients

| ref. / $\Omega^{\pi}[Nn_z\Lambda]\, n\ell_j$ | | Gareev/19/ $\beta_2 = 0.45$ | Gareev/19/ $\beta_2 = 0.35$ | Rost/21/ $\beta_2 = 0.35$ | Nilsson/20/ $\beta_2 = 0.30$ |
|---|---|---|---|---|---|
| $5/2^+$ [202] | 1d 5/2 | 1.0 | 1.0 | 0.993 | 1.0 |
| | 2s 1/2 | 0.409 | 0.498 | 0.548 | 0.37 |
| $1/2^+$ [211] | 1d 3/2 | 0.765 | 0.731 | 0.711 | 0.75 |
| | 1d 5/2 | 0.496 | 0.466 | 0.425 | 0.54 |
| | 2s 1/2 | -0.749 | -0.724 | -0.705 | -0.76 |
| $1/2^+$ [200] | 1d 3/2 | 0.587 | 0.643 | 0.665 | 0.58 |
| | 1d 5/2 | -0.294 | -0.239 | 0.222 | -0.29 |
| | 2p 1/2 | - | - | | -0.23 |
| $1/2^-$ [330] | 2p 3/2 | 0.663 | 0.632 | | 0.55 |
| | 1f 5/2 | - | - | | 0.20 |
| | 1f 7/2 | -0.734 | -0.767 | | -0.78 |

Table 4

Ratios of the calculated to the measured differential cross sections for all resolved members of rotational bands. The ratios were calculated at two angles in the forward and backward region indicated in the figures 4 - 6 and 8 by full circles. For the $1/2^-$ [330] band the deformation in the single-particle function were taken to be $\beta_2 = 0.3$, for all other bands the deformarion parameters are as indicated. The values in brackets were obtained using for the theoretical cross section the sum of the known unresolved states

| $\Omega^{\pi}[Nn_z\Lambda]$ | $J$ | forward angle $\beta_2 = 0.45$ | forward angle $\beta_2 = 0.35$ | backward angle $\beta_2 = 0.45$ | backward angle $\beta_2 = 0.35$ |
|---|---|---|---|---|---|
| $5/2^+$ [202] | 5/2 | 1.23 | | 1.20 | |
| | 7/2 | 0.83 | | 0.30 | |
| $1/2^+$ [211] | 1/2 | 0.30 | 0.45 | 0.11 | 0.18 |
| | 3/2 | 1.01 | 0.88 | 0.13 | 0.12 |
| | 5/2 | 0.87 | 0.90 | 0.21 | 0.27 |
| $1/2^+$ [200] | 1/2 | 3.5 | 3.3 | 1.55 | 0.93 |
| | 3/2 | 0.76 | 0.83 | 0.33 (0.43) | 0.32 (0.42) |
| $1/2^-$ [330] | 1/2 | 0.92 | | 0.23 | |
| | 3/2 | 2.2 | | 0.49 (0.79) | |
| | 7/2 | 0.33 (0.47) | | 0.23 (0.62) | |

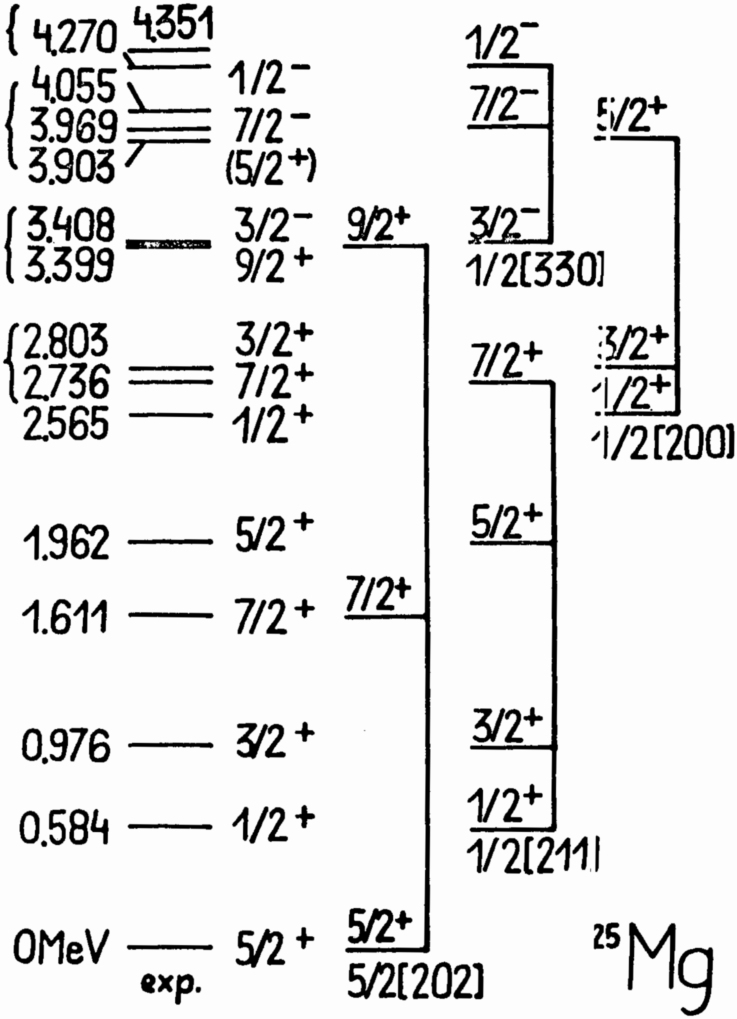


Fig. 1. Experimental level scheme of $^{25}$Mg together with the Nilsson denotation/20/. The brackets mark those levels unresolved in/12/.

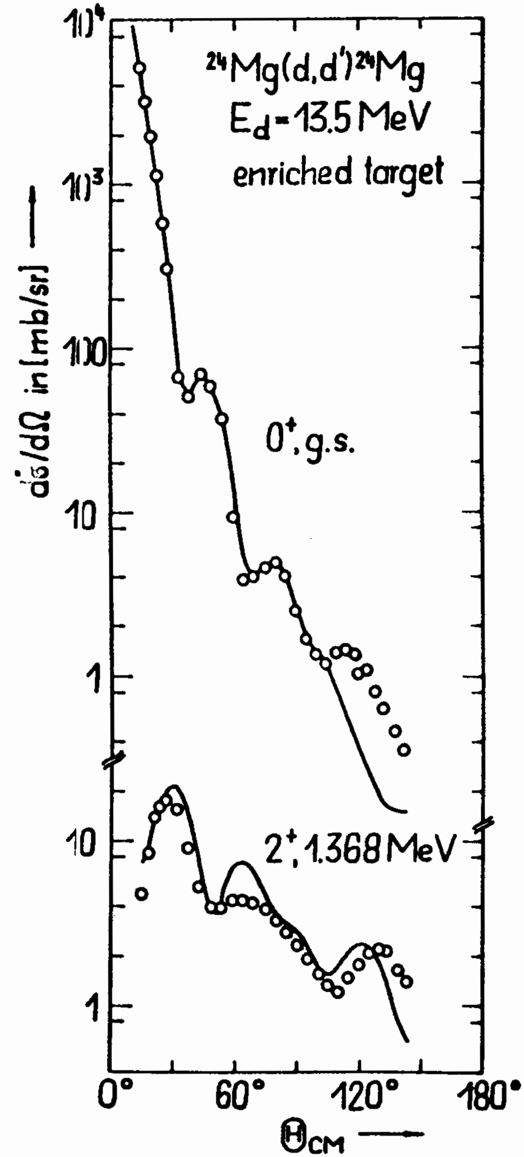


Fig. 2. Angular distributions of the $^{24}Mg(d,d')$ reaction measured by/12/ and calculated by the code KASTOR. The parameters found are compiled in table 2.

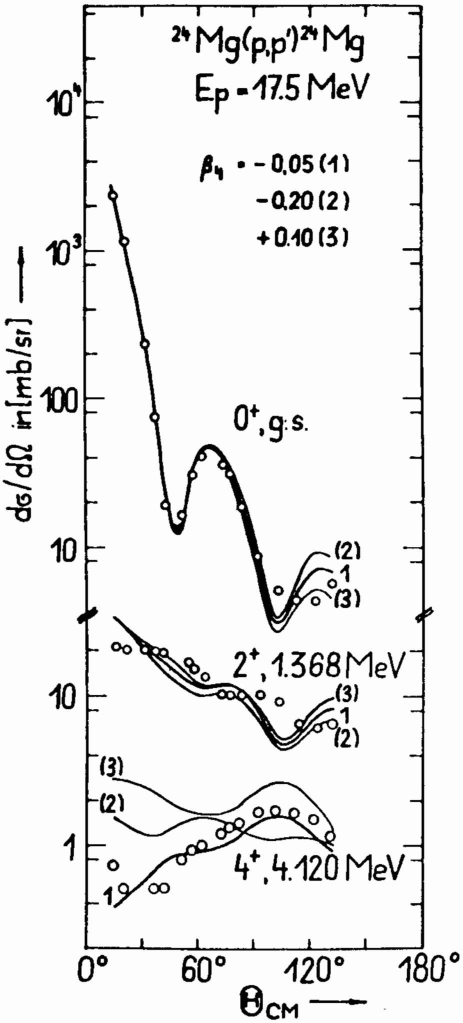


Fig. 3. Angular distributions of the $^{24}Mg(p,p')$ reaction measured by Crawley/17/ and calculated by the code KASTOR. The parameters are taken from/18/ (see table 2). The influence of $\beta_4$ is shown.

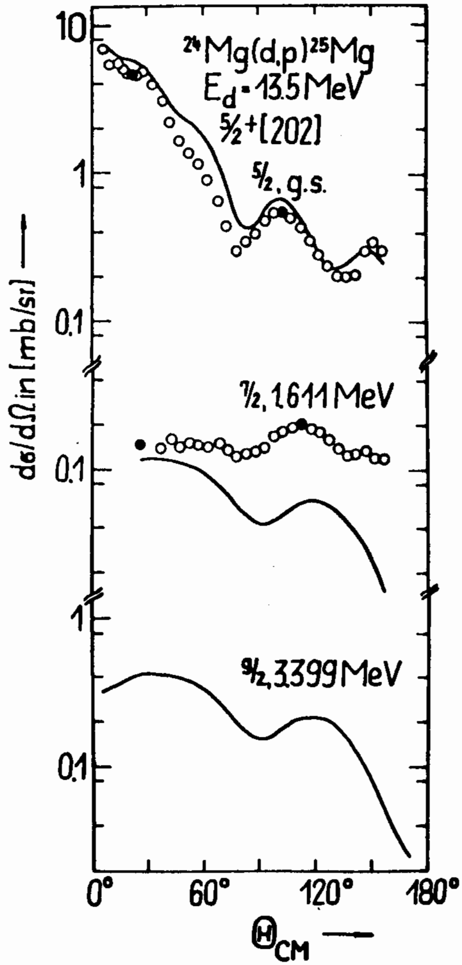


Fig. 4. Angular distributions of the $^{24}Mg(d,p)$ reaction leading to the $5/2^+$ [202] band in $^{25}Mg$. The transitions to the $7/2^+$ and $9/2^+$ states are stripping forbidden. The $9/2^+$ was not resolved from the 3/2 $1/2^-$ [330] state. The curves were calculated with the code POLLUX using the optical and deformation parameters from table 2 and the expansion coefficients obtained by Gareev and Ivanova/19/ (see table 3). The errors of the experimental data reach, only forthe weak transitions, upto about 10%, they are within the diameter of the circles for the others. The calibration error of the absolute value amounts to about 20% for each point. The full circles mark the two angles for which in table 4 the ratios $\frac{d\sigma}{d\Omega}$ (theo)/ $\frac{d\sigma}{d\Omega}$ (exp) are compiled.

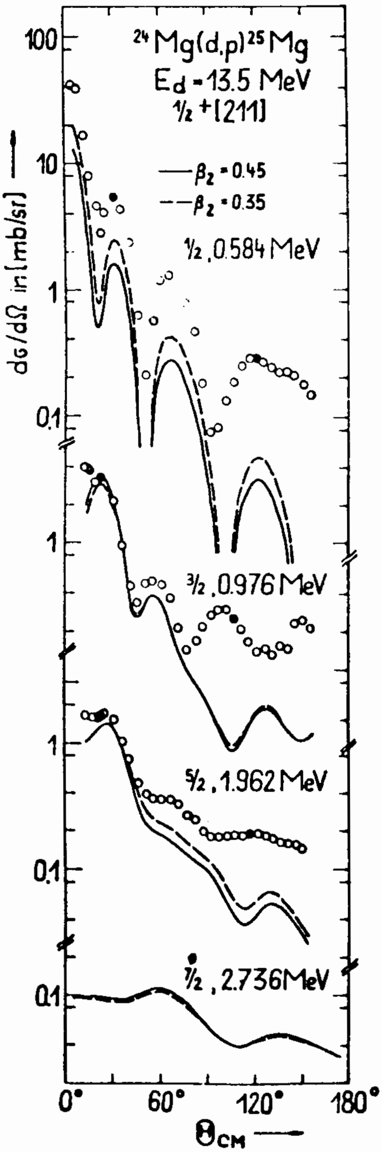


Fig. 5. Angular distributions of the $^{24}Mg(d,p)$reaction leading to the $1/2^+$ [211] band in $^{25}Mg$. The $7/2^+$ was not resolved from the 3/2 $1/2^+$ [200]. The solid lines belong to the deformation parameter for the bound state function $\beta_2$ = 0.45 and the dashed lines to $\beta_2$ = 0.35. For further explanations see fig. 4.

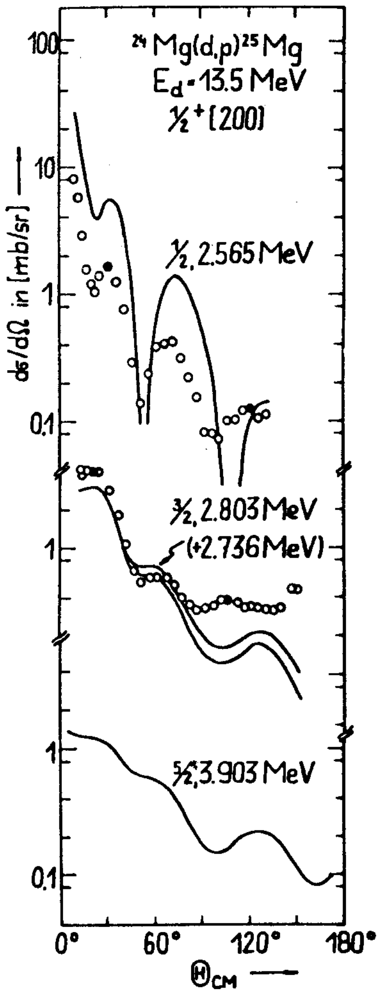


Fig, 6. Angular distributions of the $^{24}$Mg(d,p) reaction leading to the 1/2+ [200] band in $^{25}$Mg . The 3/2$^+$ state was not resolved from the weak 7/2 1/2$^+$ [211] level. The upper curve shows the sum of both calculations. For further explanations see fig. 4.

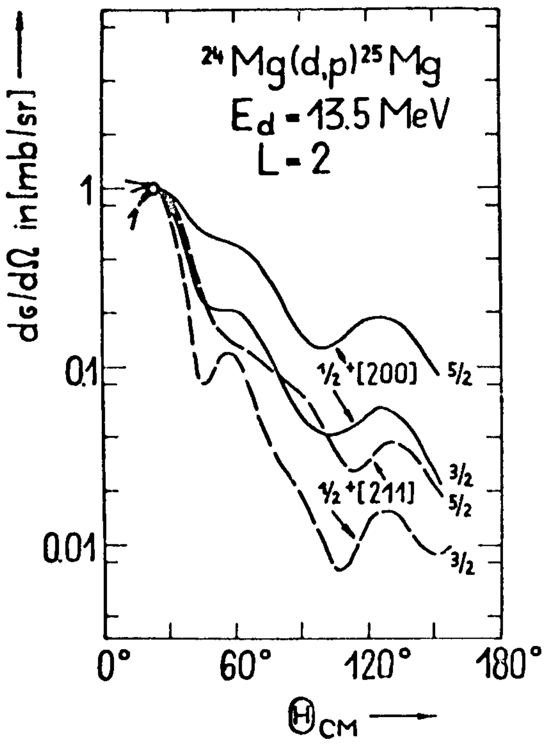


Fig. 7. Angular distributions of the L = 2 transitions to the J = 3/2 and J = 5/2 states of both the $1/2^+$ [211] and $1/2^+$ [200] bands illustrating the strong J-dependence and the dependence on the expansion coefficients $C^{(\Omega)}_{n\ell j}$ (see table 3). The curves are renormalized to each other at $\theta$ = 23°.

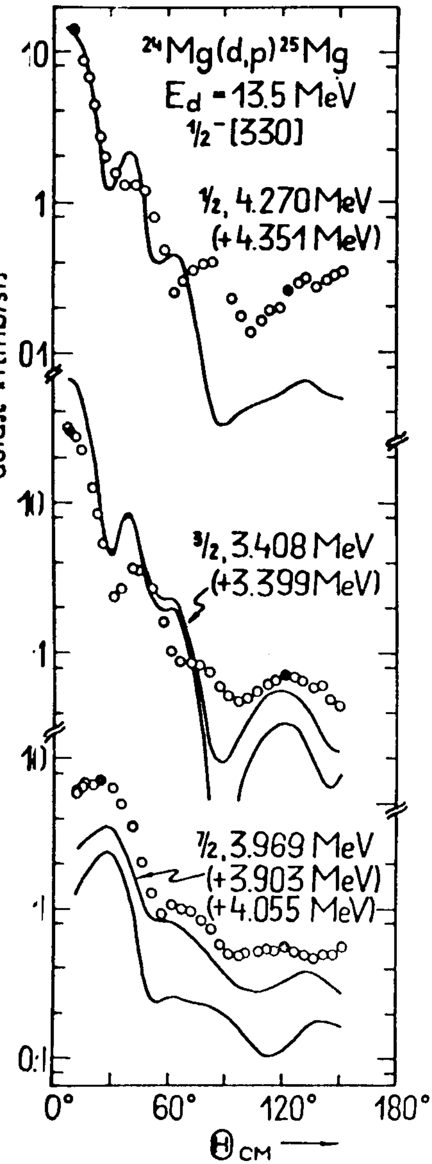


Fig. 8. Angular distributions of the $^{24}Mg(d,p)$ reaction leading to the $1/2^-$[330] band in $^{25}Mg$. No level of this band was complitely resolved from other states. The mixing levels are given in brackets. The lower curves show the calculation for the pure state of the $1/2^-$ [330] band. The upper ones give the sum of mixing states provided that their Nilsson orbit is known.